Journal of Chemical Technology and Metallurgy, 59, 6, 2024, 1421-1430

STRUCTURAL AND LUMIENESCENT STUDY OF EUROPIUM (III) DOPED TUNGSTATES

Aneliya Yordanova[1], Reni Iordanova[1], Peter Tzvetkov[1], Stancho Yordanov[2]

[1]*Institute of General and Inorganic Chemistry*
Bulgarian Academy of Sciences,
11 G. Bonchev St., Sofia 1113, Bulgaria
[2] *Bulgarian Academy of Sciences*
Institute of Metal Science
Equipment and Technologies with Hydro - and Aerodynamics Centre "Acad. A. Balevski"
67 Shipchenski prohod St., Sofia 1574, Bulgaria
E-mail: a.yordanova@svr.igic.bas.bg

Received 12 December 2023
Accepted 24 June 2024 *DOI: 10.59957/jctm.v59.i6.2024.18*

ABSTRACT

Motivated by the need of new red phosphor for white - light - emitting diodes (WLEDs) application, Eu^{3+} doped $Sc_{2-x}In_x(WO_4)_3$ (x = 0, 1, 2) solid solutions were synthesized by high temperature solid - state reaction. Structural and luminescent properties were obtained by using X - ray diffraction (XRD), infrared and photoluminescence spectroscopic techniques. IR spectrum of the $ScIn(WO_4)_3$ doped with Eu^{3+} contains the characteristic vibrations of the WO_4 and MeO_6, (Me = Sc, In) polyhedral, building the $Sc_2(WO_4)_3$ and $In_2(WO_4)_3$ structures. An effective energy transfer from the tungstate matrix to the active Eu^{3+} ion was observed. Intense red luminescence was obtained in these samples under excitation at 394 nm using the sharp $^7F_0 \rightarrow {}^5L_6$ transition of Eu^{3+}. The calculated asymmetric ratio ($^5D_0 \rightarrow {}^7F_2 / {}^5D_0 \rightarrow {}^7F_1$) was about 7.5, suggesting that the obtained materials are characterized with distorted environment around the rare earth ion and with high red emission intensity. The prepared $ScIn(WO_4)_3$ solid solution demonstrates the highest emission intensity. The obtained chromaticity coordinates of the Eu^{3+} doped $Sc_{2-x}In_x(WO_4)_3$ solid solutions were very close to the red standard recommended by National Television Standards Committee (NTSC).

Keywords: europium (III), tungstate solid solutions, X - ray diffraction, Infrared spectral analysis, luminescent properties

INTRODUCTION

Currently, white - light - emitting diodes (WLEDs) are gradually replacing conventional light sources owing to their advantages, including safety, high stability, eco - friendly nature, low power consumption, high energy efficiency and long operational lifetime [1]. The most common way to produce white light is by the combination of blue LED (InGaN) and yellow emitting material (YAG:Ce^{3+}) [2 - 5]. However, this phosphor shows low colour rendering index (CRI) (approximately 60 - 70) as there are only two - colour components in its generated white light (lack of red component). Therefore, recently more investigations are focused on the another way to obtain white light by using near UV (around 400 nm) InGaN - based LED chip, coated with tricolor phosphor, such as ZnS:Cu^+, Al^{3+} for green color [6], $BaMgAl_{10}O_{17}$:Eu^{2+} for blue colour [7], and Y_2O_2S: Eu^{3+} for red [8]. However, the red emitting component Y_2O_2S: Eu^{3+}, shows eight times lower fluorescent efficiency than that of green and blue one and it is necessary to use a phosphor mixture of 80 % red colour, 10 % green colour and 10 % blue colour to obtain good colour rendering index. Moreover, Y_2O_2S: Eu^{3+} is unstable under excitation of high - energy UV photons, which may cause an environmental pollution due to release of sulfide gas. Thus, the development of red - emitting phosphor with good chemical and thermal stability, high efficiency and appropriate CIE (International Commission on Illumination) chromaticity coordinates upon near-UV excitation is urgently needed.

A typical activator for red - emitting phosphors is the Europium (III) ion. Eu^{3+} should be embedded in matrices, which can provide lattice sites with low symmetry and/or with strong covalent interaction between active ion and the surrounding anions to obtain intense red $^5D_0 \rightarrow {}^7F_2$ photoluminescence. To gain strong covalent bonding, the activator ions should be incorporated onto small lattice sites, for example by substituting Ga^{3+}, Sc^{3+}, In^{3+}, Y^{3+} ions, with low coordination number, i.e. six or eight. The main drawback of Eu^{3+} ion is the weak intensity of its spin and parity-forbidden f - f transitions, which inhibit achieving high excitation and emission efficiency of the red luminescence. One of the ways to improve the Eu^{3+} excitation is to find suitable host materials with strong absorption in the ultraviolet region and ability to effectively transfer the absorbed energy to the active center, which should result in an enhanced emission intensity (host sensitized luminescence). Tungstates and molibdates phases are very appropriate for hosting Eu^{3+} active ions as their strong absorption associated to the charge transfer within the $[WO_n]$ and $[MoO_n]$ units are situated in the 250 - 350 nm spectral region [9, 10]. Along with this, the emission band of WO_4 groups (broad band between 400 nm and 600 nm) overlaps the excitation peaks of Eu^{3+}, which is the requirement for energy transfer.

In this work we study the luminescence properties of the Eu^{3+} doped $Sc_{2-x}In_x(WO_4)_3$ solid solutions and compare their emission intensities and CIE coordinates with other studied tungstate luminescent materials and the commercially used red phosphors: Y_2O_2S: Eu^{3+} and Y_2O_3:Eu^{3+}.

EXPERIMENTAL

The 1 at. % Eu^{3+} doped $Sc_{2-x}In_x(WO_4)_3$ (x = 0, 1, 2) solid solutions were synthesized by the traditional high temperature solid - state reaction. As initial materials were used Sc_2O_3, In_2O_3, WO_3 and Eu_2O_3, with a purity at least 99.9 %. The reactant substances were weighed according to their stoichiometric ratio and then ground thoroughly in an agate mortar for 30 min to achieve the proper mixing. Subsequently, the samples were transferred to platinum crucibles and heated at 900°C for 6 h in air to mix them uniformly and then sintered at 1100°C for 24 h. After cooling down, the samples were ground into powder and were collected for measurements.

Structural characterization was carried out by powder XRD using a Bruker D8 Advance powder diffractometer with Cu Kα radiation and SolX detector. XRD spectra were recorded at room temperature. Data were collected in the 2θ range from 10° to 50° with a step 0.04° and 1 s/step counting time. XRD spectra were identified using the Diffractplus EVA program. The obtained data were used for determining the lattice parameters of the solid solution. The IR spectra of the samples were recorded in the 1100 - 400 cm^{-1} region, using the KBr pellet technique (Nicolet - 320 FT-IR spectrometer). Photoluminescence (PL) excitation and emission spectra were measured with a PL spectrometer (Scinco FS - 2 with wavelength accuracy 1 nm) at room temperature.

RESULTS AND DISCUSSION

X-ray diffraction (XRD)

The diffraction peaks of the prepared solid solutions for x = 2.0 ($In_2(WO_4)_3$) and 1.0 ($ScIn(WO_4)_3$) match exactly those of the monoclinic symmetry with space group P21/a [ICDD No. 74-4413], while for x value equals to 0 ($Sc_2(WO_4)_3$) corresponds to the orthorhombic symmetry, space group Pnca [ICDD No. 21-1065] [11, 12]. As pointed out in the literature data, both structures are close to each other and their X - ray pattern differ mainly in the two additional peaks for the monoclinic $In_2(WO_4)_3$ at 2θ = 23.6 and 25.7 (Fig. 1b). No other diffraction peaks from impurities are registered. As can be seen from figure 1b, a slight shift of peaks at higher 2θ values with increasing Indium content is observed, which is a proof that single - phase Eu^{3+} doped $Sc_{2-x}In_x(WO_4)_3$ solid solutions are synthesized.

The calculated lattice parameters of the undoped $Sc_{2-x}In_x(WO_4)_3$ and Eu^{3+} doped $Sc_{2-x}In_x(WO_4)_3$ solid solutions are shown in Table 1 [13]. Because of the similarity of the ionic radii of Scandium (0.745 Å), Indium (0.8 Å) and Europium (0.947 Å), it is expected

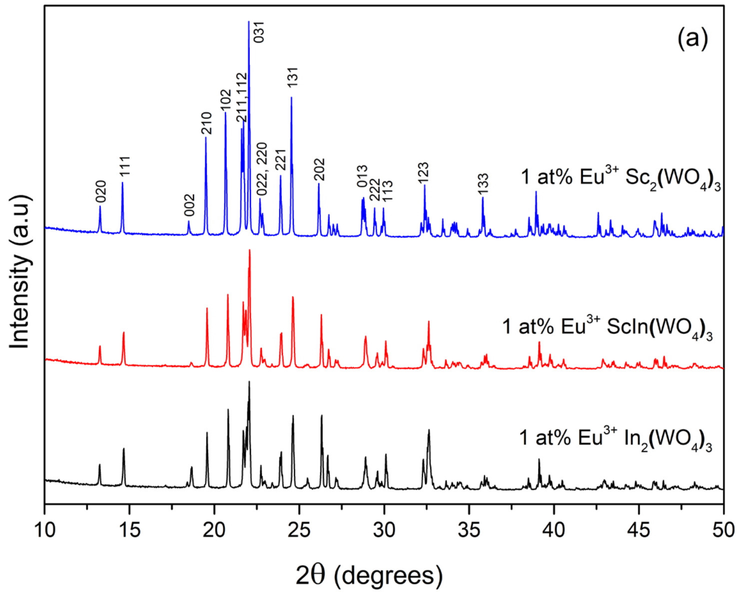

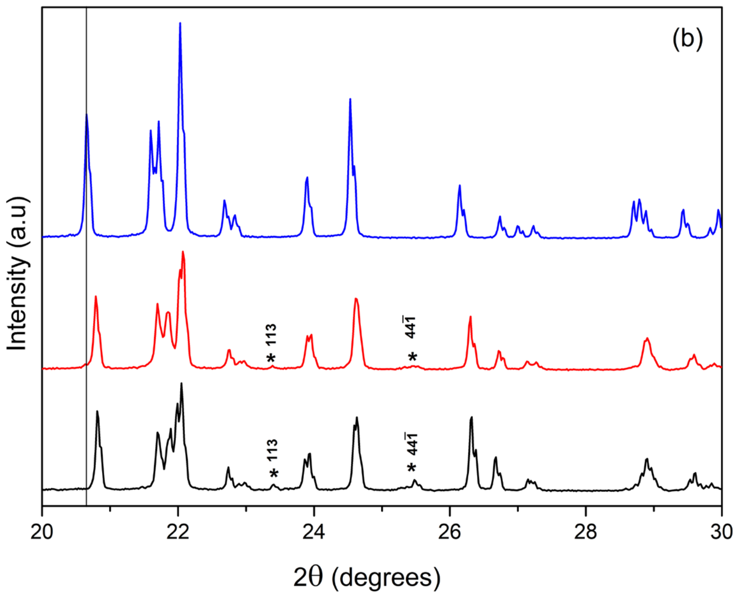

Fig. 1. (a) X - ray diffraction patterns of 1 at. % Eu^{3+} doped $Sc_{2-x}In_x(WO_4)_3$ (x = 0, 1, 2); (b) The same X - ray pattern (narrow scale) with marked picks (*) corresponding to the monoclinic symmetry with space group P21/a in the case of x = 1.0 and 2.0.

Table 1. Cell parameters a, b, c, angle and cell volume, V of non - doped $Sc_{2-x}In_x(WO_4)_3$ and of 1 at. % Eu^{3+} doped $Sc_{2-x}In_x(WO_4)_3$ solid solutions.

Solid solution composition	a, Å	b, Å	c, Å	beta, °	V, Å^3	Symmetry	Reference
$Sc_2(WO_4)_3$	9.677	13.325	9.586	90	1236.1	Pnca	[13]
$Sc_2(WO_4)_3$: 1 at. % Eu^{3+}	9.682	13.332	9.592	90	1238.1	Pnca	Current work
$ScIn(WO_4)_3$	16.355	9.637	19.038	125.38	2446.5	P21/a	[13]
$ScIn(WO_4)_3$: 1 at .% Eu^{3+}	16.364	9.659	19.073	125.44	2456.1	P21/a	Current work
$In_2(WO_4)_3$	16.375	9.638	19.039	125.31	2452.2	P21/a	[13]
$In_2(WO_4)_3$: 1 at. % Eu^{3+}	16.376	9.644	19.030	125.31	2452.3	P21/a	Current work

Eu^{3+} to easily enter the host lattice and to substitute both Sc^{3+} and In^{3+} sites. The slight increase of the lattice parameters and cell volume with Eu^{3+} doping is evidence that the active ion is embedded in the host lattices.

Infrared spectral analysis

Fig. 2 shows IR spectra of the obtained samples $Sc_{2-x}In_x(WO_4)_3$ (x = 0, 1, 2) doped with 1 at. % Eu^{3+}. The shape of the spectrum of the solid solution $ScIn(WO_4)_3$ (x = 1) and band positions are similar with the spectra of $Sc_2(WO_4)_3$ and $In_2(WO_4)_3$ which is indicating that the short - range order of obtained solid solution resembles those of $Sc_2(WO_4)_3$ and $In_2(WO_4)_3$ [14, 15]. The strong bands in the spectral range between 900 and 800 cm^{-1} are due to asymmetric stretching vibrations (ν_{as}) of WO_4 structural units. The appearance of several absorption bands in this area is due to splitting of the asymmetric vibrations of highly distorted WO_4 groups. The bands assigned above 900 cm^{-1} are owing to symmetric stretching vibrations (ν_s) of crystallographically non - equivalent WO_4 tetrahedra with different local symmetry, present in these structures [15, 16].

Photoluminescent properties

The excitation spectra of Eu^{3+} doped $Sc_{2-x}In_x(WO_4)_3$ (x = 0, 1, 2) were registered monitoring the $^5D_0 \rightarrow {}^7F_2$ emission of Eu^{3+} at 615 nm (Fig. 3). In the spectral region from 200 to 600 nm, a highly intensive broad band with maximum at 250 nm and several sharp bands with low intensity are observed. The broad band is attributed to the ligand to metal charge transfer states (LMTC) associated with energy transfer from $O^{2-} \rightarrow W^{6+}$ in WO_4 groups and $O^{2-} \rightarrow Eu^{3+}$ transitions [9, 10, 17 - 19]. The presence of strong absorption of WO_4 groups monitoring the red emission of Eu^{3+} at 615 nm indicates that the energy absorbed by tungstate groups can be transmitted non - radiatively to Eu^{3+}. As a result, an increase in the emission intensity of the active ion is expected to occur (host sensitized luminescence). The low intensity absorption peaks in spectral range 320 - 600 nm are attributed to the typical intra - configurational f - f forbidden transitions of Eu^{3+} within its {Xe}$4f^6$ configuration: $^7F_0 \rightarrow {}^5H_3$, $^7F_0 \rightarrow {}^5D_4$, $^7F_0 \rightarrow {}^7L_7$, $^7F_0 \rightarrow {}^5L_6$, $^7F_0 \rightarrow {}^5D_3$, $^7F_0 \rightarrow {}^5D_2$, $^7F_0 \rightarrow {}^5D_1$, $^7F_0 \rightarrow {}^5D_0$ at 320 nm, 362 nm, 382 nm, 394 nm,

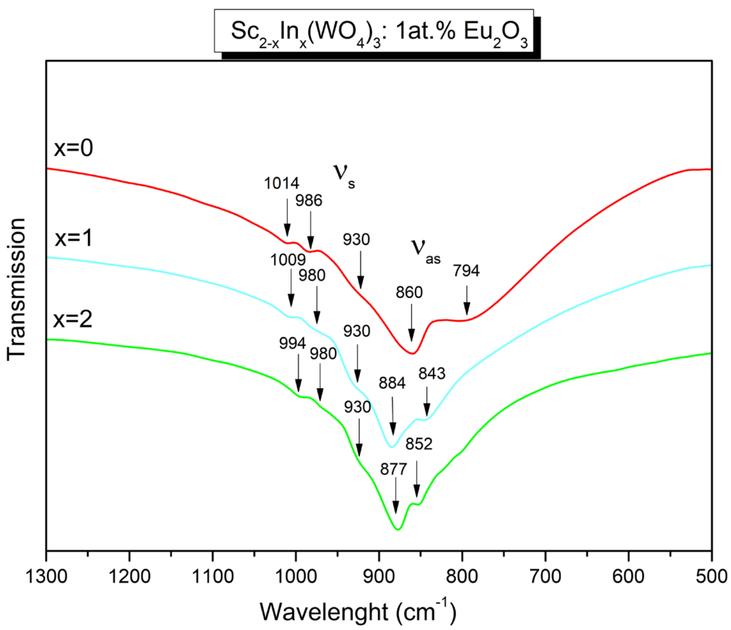

Fig. 2. Infrared spectra of the 1 at. % Eu^{3+} doped $Sc_{2-x}In_x(WO_4)_3$ (x = 0, 1, 2).

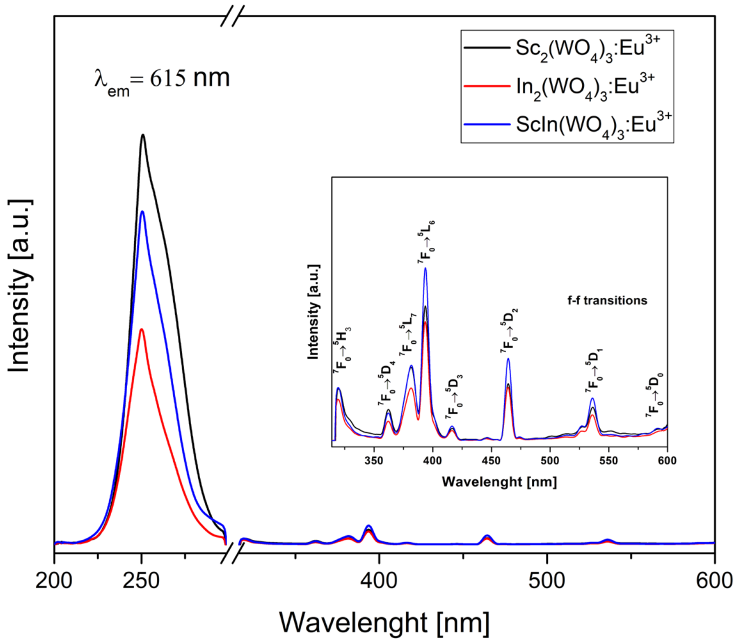

Fig. 3. Excitation spectra of 1 at. % Eu^{3+} doped $Sc_{2-x}In_x(WO_4)_3$ (x = 0, 1, 2).

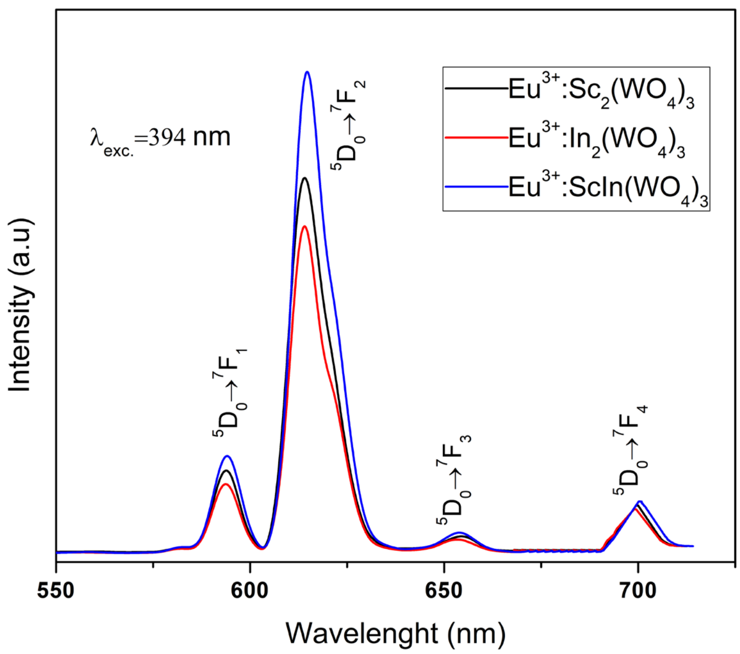

Fig. 4. Emission spectra of 1 at. % Eu^{3+} doped $Sc_{2-x}In_x(WO_4)_3$ (x = 0, 1, 2).

416 nm, 464 nm, 536 nm and 594 nm, respectively. Their low intensity is due to the fact that they are forbidden by the Laporte`s selection rule [20]. Among them, the most dominant band is registered at 394 nm and was used as an excitation wavelength to record the emission spectra.

The emission spectra of Eu^{3+} doped $Sc_{2-x}In_x(WO_4)_3$ (x = 0, 1, 2) solid solutions are shown on Fig. 4. Under the excitation of 394 nm, the emission spectra are composed of identical intra-configurational transitions of Eu^{3+} ions from $^5D_0$ to ^7F_J (J = 1, 2, 3 and 4) states at 594 nm, 615 nm, 653 nm and 700 nm, respectively. According to the literature data in the spectral region 400 - 600 nm is registered the broad emission band of

WO_4 group [21]. In the same spectral range are located the excitation bands of Eu^{3+} shown at Fig. 3. The main requirement for energy transfer from the host material to the luminescent ion is the existence of a spectral overlap between the emission band of the corresponding matrix and the excitation band of the active ion embedded in it. In the studied materials, this condition is fulfilled. Furthermore, evidence of the occurrence of the energy transfer is the absence of emission band of WO_4 in the emission spectra [10, 22, 23]. Thus, all the absorbed energy by the host has been transferred non - radiatively to the activator Eu^{3+} by quenching its luminescence. This was previously also established by as for tungstate - containing glass materials [22 - 24].

The most intensive electronic transition located at 615 nm is attributed to the $^5D_0 \rightarrow {}^7F_2$ transition of the europium ion. The other transitions in the emission spectra are characterized with low intensity, which is favourable for obtaining a red emitting luminescent material with high colour purity. Generally, the integrated emission intensity ratios (R) of the electric dipole to a magnetic dipole transition ($^5D_0 \rightarrow {}^7F_2/{}^5D_0 \rightarrow {}^7F_1$) is often used as a measure for evaluating the symmetry condition of the coordination environment around Eu^{3+} ions. When the Eu^{3+} ion is located at a low symmetry site the $^5D_0 \rightarrow {}^7F_2$ transition is predominant, while if it is located in high symmetry sites the $^5D_0 \rightarrow {}^7F_1$ will dominate the emission spectra. In this way, R value provides information about the red ($^5D_0 \rightarrow {}^7F_2$) colour richness in comparison with the orange ($^5D_0 \rightarrow {}^7F_1$) colour. Samples with large value of the luminescence intensity ratio (R) show a high degree of asymmetry around the Eu^{3+} ions and a high intensity of red emission [25, 26].

In the synthesized Eu^{3+} doped $Sc_{2-x}In_x(WO_4)_3$, the red emission is more intensive than the orange one and the calculated R values are in range 7.36 - 7.58 (Table 2). The R values are higher than most of other reported Eu^{3+} doped tungstates in the literature, and higher compared to the most common commercially applied red phosphors: Eu^{3+} doped Y_2O_3 and Eu^{3+} doped Y_2O_2S, suggesting

Table 2. Comparison of the luminescence intensity ratio (R) of $^5D_0 \rightarrow {}^7F_2$ to $^5D_0 \rightarrow {}^7F_1$ transition of Eu^{3+} - doped tungstates and the commercially used red phosphors.

Sample composition	R values	References
$Sc_2(WO_4)_3$: 1 at. % Eu^{3+}	7.39	Current work
$In_2(WO_4)_3$: 1 at. % Eu^{3+}	7.36	Current work
$ScIn(WO_4)_3$: 1 at. % Eu^{3+}	7.58	Current work
$LiGd(WO_4)_2$: xEu (x=0.01 - 0.11)	1.53 - 1.59	[27]
$Eu_xY_{6-x}WO_{12}$(x=0.1 - 1.0)	~2	[28]
$Th(WO_4)_2$: 2.0 mol % Eu^{3+}	3.27	[29]
$BaLa_{2-x}Eu_xWO_7$ (x = 0.01 - 0.40)	3.55 - 4.15	[30]
$Li_3BaSrLa_{3-x}Eu_x(WO_4)_8$ (x = 0 - 3)	3.07 - 8.47	[31]
Eu^{3+}:$NaGd(WO_4)_2$	6.05 - 8.79	[32]
$CaWO_4$: 1 mol % Eu^{3+} $SrWO_4$: 1mol % Eu^{3+}	6.6 6.8	[33]
$Na_{1-x}Li_xLa_{0.95}Eu_{0.05}(WO_4)$ (x = 0 - 6.03)	7.35 - 7.81	[34]
40 at. % Eu^{3+}: $KLa(WO_4)_2$	7.87	[35]
$PbLa_{1.13}Eu_{0.88}(WO_4)_4$	9	[36]
$Li_3Ba_2Y_{3-x}Eu_x(WO_4)_8$ (x = 0.1, 1, 1.5, 2 and 2.8)	~9.5	[37]
Eu_x:$RbGd_{(1-x)}(WO_4)_2$ (x = 0.8)	10	[38]
Eu^{3+} doped Y_2O_2S	6.4 - 5.6	[39]
Eu^{3+} doped Y_2O_3:Eu^{3+}	3.8 - 5.2	[40, 41]

that the obtained materials are characterized with more distorted environment around the rare earth ion and with high luminescence [27 - 41]. The highest value of asymmetric ratio and the highest emission intensity belongs to $ScIn(WO_4)_3$ (x = 1), where the active ion can occupy two different sites with low symmetry in the lattice - of Scandium and Indium.

CIE color chromaticity coordinates and comparison of Eu^{3+} doped $Sc_{2-x}In_x(WO_4)_3$ (x = 0, 1, 2) with $Y_2O_3:Eu^{3+}$, $Y_2O_2S:Eu^{3+}$ and NTSC standard for red colour

To characterize the emission color of Eu^{3+} doped $Sc_{2-x}In_x(WO_4)_3$, the standard Commission International de l'Eclairage (CIE) 1931 chromaticity diagram was used [42]. From the luminescence spectra, the chromaticity coordinates of specimens were calculated using color calculator software. As can be seen from Table 3, the values are in the red region of the CIE diagram, and they are very close to the standard recommended by NTSC than to the commercially applied $Y_2O_3:Eu^{3+}$ [8] and $Y_2O_2S:Eu^{3+}$ [43]. The calculated coordinates are almost identical and cannot be individually separated on CIE diagram (Fig. 5). This data show that the obtained tungstates are emitting red color with high purity.

CONCLUSIONS

In summary, Eu^{3+} doped $Sc_{2-x}In_x(WO_4)_3$ (x = 0, 1, 2) solid solutions were synthesized by solid-state method. Results from XRD analysis indicate that single phase

Table 3. CIE chromaticity coordinates of Eu^{3+} doped $Sc_{2-x}In_x(WO_4)_3$ solid solutions.

Sample composition	Chromaticity coordinates (x,y)
$Sc_2(WO_4)_3$: 1 at. % Eu^{3+}	(0.648, 0.349)
$In_2(WO_4)_3$: 1 at. % Eu^{3+}	(0.650, 0.348)
$ScIn(WO_4)_3$: 1 at. % Eu^{3+}	(0.656, 0.342)
NTSC standard for red color	(0.670, 0.330)
$Y_2O_2S:Eu^{3+}$	(0.658, 0.340)
Y_2O_3: Eu^{3+}	(0.644, 0.358)

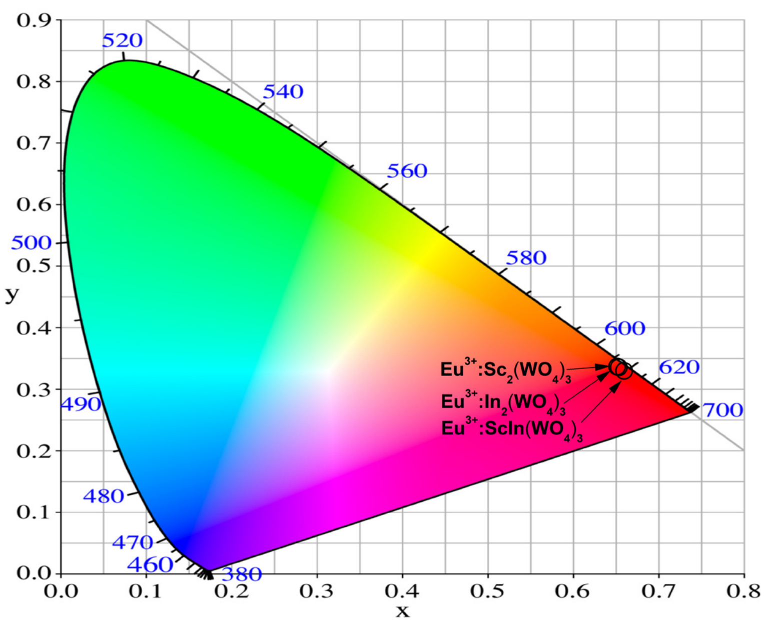

Fig. 5. CIE chromaticity diagram of the 1 at. % Eu^{3+} doped $Sc_{2-x}In_x(WO_4)_3$, (x = 0, 1, 2).

compounds are obtained and the Eu^{3+} ion is embedded in the host lattices. The obtained solid solutions possess monoclinic symmetry with space group P21/a for x value 2.0 and 1.0 and orthorhombic symmetry, space group Pnca for x value of 0. All IR spectra contain the characteristic vibrations of WO_4 and MeO_6 (Me = Sc or In) polyhedra, building the structure of these crystalline phases. The obtained solid solutions display intense red luminescence under excitation at 394 nm, because of the occurred non - radiative energy transfer from host lattice to the active ion (host sensitized luminescence). $ScIn(WO_4)_3$ (x = 1) possesses the highest emission intensity, as in this structure the active ion occupy sites with lowest symmetry. The calculated CIE chromaticity coordinates were very close to the values of the standard red color, recommended by NTSC.

These results show that Eu^{3+} doped $Sc_{2-x}In_x(WO_4)_3$ solid solutions could find application as high purity red - emitting phosphors for white light emitting diodes.

Acknowledgments

Special thanks are due to Nikolai I. Georgiev for Photoluminescent measurements.

REFERENCES

1. J. Cho, J.H. Park, J.K. Kim, E.F. Schubert, White light-emitting diodes: History, progress, and future, Laser Photonics Rev., 11, 2017, 1600147.
2. S. Nakamura, G. Fasol, The blue laser diode: GaN based light emitters and lasers, Heidelberg, Springer Science & Business Media, 2013.
3. Y. Shimizu, K. Sakano, Y. Noguchi, T. Moriguchi, U.S. Pat. 5998925, 1998.
4. Y. Sang, H. Liu, Y. Lv, J. Wang, T. Chen, D. Liu, X. Zhang, H. Qin, X. Wang, R.I. Boughton, J. Alloys Compd., 490, 2010, 459-462.
5. R. Praveena, L. Shi, K. H. Jang, V. Venkatramu, C.K. Jayasankar, H.J. Seo, J. Alloys Compd., 509, 2011, 859-863.
6. Y. Chen, J. Duh, B. Chiou, C. Peng, Luminescent mechanisms of ZnS: Cu: Cl and ZnS: Cu: Al phosphors, Thin Solid Films, 392, 1, 2001, 50-55.
7. K. Kim, Y. Kim, H. Chun, T. Cho, J. Jung, J. Kang, Structural and optical properties of $BaMgAl_{10}O_{17}$: Eu^{2+} phosphor, Chem. Mater., 14, 12, 2002, 5045-5052.
8. S. Trond, J. Martin, J. Stanavage, A. Smith, Properties of Some Selected Europium-Activated Red Phosphors, J. Electrochem. Soc., 116, 7, 1969, 1047-1050.
9. G. Blasse, B.C. Grabmaier, Luminescent Materials, VerJag Berlin Heidelberg, Springer, 1994, 18.
10. P.S. Dutta, A. Khanna, Eu^{3+} Activated Molybdate and Tungstate Based Red Phosphors with Charge Transfer Band in Blue Region, ECS J. Solid State Sci Technol., 2, 2013, R3153-R3167.
11. V. Sivasubramanian, T.R. Ravindran, R. Nithya, A.K. Arora, Structural phase transition in indium tungstate, J. Appl. Phys., 96, 2004, 387-392.
12. J.S.O. Evans, T.A. Mary, A.W. Sleight, Negative thermal expansion in $Sc_2(WO_4)_3$, J. Solid State Chem., 137, 1998, 148-160.
13. A.S. Yordanova, R.S. Iordanova, V.S. Nikolov, I.I. Koseva, P.T. Tzvetkov, Bulg. Chem. Commun., 49 A, 2017, 91.
14. M. Maczka, K. Hermanowicz, A. Pietraszko, A. Yordanova, I. Koseva, Structure, optical and phonon properties of bulk and nanocrystalline $Al_{2-x}Sc_x(WO_4)_3$ solid solutions doped with Cr^{3+}, Opt. Mater., 36, 2014, 685-664.
15. M. Maczka, K. Hermanowic, J. Hanuza, Phase transition and vibrational properties of $A_2(BO_4)_3$ compounds (A= Sc, In; B= Mo, W), J. Mol. Struct., 744, 2005, 283-288.
16. K. Nakamoto, Infrared and Raman Spectra of Inorganic and Coordination Compound, New York, Wiley, 1997.
17. H.E. Hoefdraad, The charge-transfer absorption band of Eu^{3+} in oxides, J. Solid State Chem., 15, 2, 1975, 175–177.
18. A.K. Parchur, R.S. Ningthoujam, Behaviour of electric and magnetic dipole transitions of Eu^{3+}, $^5D_0 \rightarrow {}^7F_0$ and Eu–O charge transfer band in Li^+ co-doped YPO_4:Eu^{3+}, *RSC Adv.*, *2*, 2012, 10859-10868.
19. K. Mariselvam, L. Juncheng, Synthesis and luminescence properties of Eu^{3+} doped potassium titano telluroborate (KTTB) glasses for red laser applications, J. Lumin, 230, 2021, 117735.
20. J.C.G. Bünzli, Lanthanide luminescence: from a mystery to rationalization, understanding, and applications, Handbook on the Physics and Chemistry

of Rare Earths, Elsevier, 50, 2016, 141-176.
21. J. Sungpanich, T. Thongtem, S. Thongtem, Large-scale synthesis of WO_3 nanoplates by a microwave-hydrothermal method, Ceram. Int., 38, 2, 2012, 1051-1055.
22. M. Milanova, L. Aleksandrov, A. Yordanova, R. Iordanova, N. S. Tagiara, A. Herrmann, G. Gao, L. Wondraczek, E.I. Kamitsos, Structural and luminescence behavior of Eu^{3+} ions in ZnO-B_2O_3-WO_3 glasses, J. Non-Cryst. Solids, 600, 2023, 122006.
23. L. Aleksandrov, A. Yordanova, M. Milanova, R. Iordanova, M. Fabian, Doping effect of WO_3 on the structure and luminescent properties of ZnO-B_2O_3-Bi_2O_3:Eu^{3+} glass, J. Chem. Technol. Metall., 58, 4, 2023, 707-715.
24. A. Yordanova, M. Milanova, R. Iordanova, M. Fabian, L. Aleksandrov, P. Petrova, Network Structure and Luminescent Properties of ZnO–B_2O_3–Bi_2O_3–WO_3:Eu^{3+} Glasses, Materials, 16, 20, 2023, 6779.
25. C.B.A. Devi, Sk. Mahamuda, K. Swapna, M. Venkateswarlu, A. Srinivasa Rao, G. Vijaya Prakash, Compositional dependence of red luminescence from Eu^{3+} ions doped single and mixed alkali fluoro tungsten tellurite glasses, Opt. Mater., 73, 2017, 260-267.
26. R. Reisfeld; E. Zigansky, M. Gaft, Europium probe for estimation of site symmetry in glass films, glasses and crystals, Mol. Phys., 102, 2004,1319-1330.
27. D.L. Shruthi, A.J. Reddy, G.A. Kumar, C.K. Jayasankar, Judd Ofelt theoretical analysis, photoluminescence properties of Eu^{3+} activated $LiGd(WO_4)_2$ phosphors, Journal of luminescence, 222, 2020, 117167.
28. T.C. Chien, J.C. Yang, C.S. Hwang, M. Yoshimura, Synthesis and photoluminescence properties of red-emitting Y_6WO_{12}: Eu^{3+} phosphors, Journal of Alloys and Compounds, 676, 2016, 286-291.
29. M. Keskar, S.K. Gupta, R. Phatak, S. Kannan, V. Natarajan, Optical properties of Eu^{3+} activated thorium molybdate and thorium tungstate: Structure, local symmetry and photophysical properties, Journal of Photochemistry and Photobiology A: Chemistry, 311, 2015, 59-67.
30. S.A. Yan, Y.S. Chang, W.S. Hwang, Y.H. Chang, M. Yoshimura, C.S. Hwang, Synthesis and photoluminescence properties of color-tunable $BaLa_2WO_7$: Eu^{3+} phosphor, Journal of Alloys and Compounds, 509, 19, 2011, 5777-5782.
31. K. Singh, S. Vaidyanathan, $Li_3BaSrLa_3(WO_4)_8$:Eu^{3+} and Its Solid Solutions: A New Red Emitting Phosphor-Structure, Synthesis and Appraisal of Optical Properties, Chemistry Select, 2, 18, 2017, 5143-5156.
32. W.A.N.G. Yeqing, T.A.N.G. Jieqin, X. Huang, L. Jiang, Luminescence properties of Eu^{3+}: $NaGd(WO_4)_2$ nanoparticles and nanorods, Journal of Rare Earths, 34, 2, 2016, 118-124.
33. B.S. Barros, A.C. De Lima, Z.R. Da Silva, D.M.A. Melo, S. Alves-Jr, Synthesis and photoluminescent behavior of Eu^{3+}-doped alkaline-earth tungstates, Journal of Physics and Chemistry of Solids, 73, 5, 2012, 635-640.
34. Y. Liu, Z. G. Lu, Y. Y. Gu, W. Li, Hydrothermal-assisted ion exchange synthesis and photoluminescence of Li^+ and Eu^{3+} co-doped $NaLa(WO_4)_2$ as near-UV type red phosphors, Journal of luminescence, 132, 5, 2012, 1220-1225.
35. K.K. Rasu, D. Balaji, S.M. Babu, Spectroscopic properties of Eu^{3+}: $KLa(WO_4)_2$ novel red phosphors, Journal of Luminescence, 170, 2016, 547-555.
36. A.S. Altowyan, A. Hammoud, A.V. Lebedev, S.A. Avanesov, L.V. Vasileva, V.A. Klimenko, M.S. Al-Buriahi, Synthesis and properties of novel Pb/La/WO_4: Eu^{3+} red phosphors for white light emitting diodes (WLEDs), Optik, 268, 2012, 169805.
37. L. Wang, W. Guo, Y. Tian, P. Huang, Q. Shi, High luminescent brightness and thermal stability of red emitting $Li_3Ba_2Y_3(WO_4)_8$: Eu^{3+} phosphor, Ceramics International, 42, 12, 2016, 13648-13653.
38. K.K. Rasu, D. Balaji, S.M. Babu, Photoluminescence properties of Eu^{3+}:$RbGd(WO_4)_2$ red phosphors prepared by sol–gel method, Journal of Luminescence, 170, 3, 2016, 825-834.
39. S. Som, P. Mitra, V. Kumar, V. Kumar, J.J. Terblans, H.C. Swart, S.K. Sharma, The energy transfer phenomena and colour tunability in Y_2O_2S: Eu^{3+}/Dy^{3+} micro-fibers for white emission in solid state lighting applications, Dalton Trans., 43, 2014, 9860-9871.
40. H. Song, B. Chen, B. Sun, J. Zhang, S. Lu, Ultraviolet light-induced spectral change in cubic nanocrystalline Y_2O_3: Eu^{3+}, Chem. Phys. Lett., 372, 3-4, 2003, 368-372.
41. M. Kabir, M. Ghahari, M.S. Afarani, Co-precipitation

synthesis of nano Y_2O_3: Eu^{3+} with different morphologies and its photoluminescence properties, Ceram. Int., 40, 7, 2014, 10877-10885.
42. T. Smith, J. Guild, The CIE colorimetric standards and their use, Trans. Opt. Soc., 33, 3, 1931, 73.
43. M. Rajendran, S. Vaidyanathan, New red emitting phosphors $NaSrLa(MO_4)_3$: Eu^{3+} [M = Mo and W] for white LEDs: Synthesis, structural and optical study, Journal of Alloys and Compounds, 789, 2019, 919-931.